SMiRT-12 / K. Kussmaul (Editor)
© 1993 Elsevier Science Publishers B.V. All rights reserved.

JH13/2

ESTIMATIONS OF IMPACT STRENGTH ON REINFORCED CONCRETE STRUCTURES BY THE DISCRETE ELEMENT METHOD

H. Morikawa, N. Kusano, N. Koshika, T. Aoyagi, Y. Hagiwara and Y. Sawamoto

Kajima Corporation, Tokyo 107, Japan

1 INTRODUCTION

There has been a rising interest in the response of reinforced concrete structures to impact loading , from the point of view in particular of disaster prevention at nuclear power facilities, and there is an urgent requirement for establishment of design methods against such type of loads.

Structural damage on reinforced concrete structures under impact load includes local damage and global damage. The behavior of local damage, such as penetration into the structures, rear face scabbing, perforation, or spalling, has been difficult to estimate by numerical analysis, but over recent years research has advantaged and various analytical methods have been tried. The authors proposed a new approach for assessing local damage characteristics by applying the discrete element method (DEM), and verified that the behavior of a concrete slab suffering local damage may be qualitatively expressed[1]. This was followed by the discussion of the quantitative evaluation of various constants used in the DEM analysis in reference [2].

The authors apply the DEM to the simulation analysis of impact tests [3] on reinforced concrete panels and analytical investigations are made on the local damage characteristics and response values that are difficult to assess through tests, in an attempt to evaluate the mechanism of local damage according to the hardness of the missiles.

2 BASIC CONCEPT OF DEM

The DEM idealizes the concrete/steel medium to comprise an assemblage of particles, each particle having to satisfy equations of motion, and the dynamic characteristics of the whole body being expressed by the forces transferred between particles during contact. Elements of circular form are used in the method, with forces between elements expressed by springs and dashpots aligned in the normal and shear directions. Interactive conditions include the incorporation of simple bonding and non-linear interaction forces resulting from the fracture criteria. Spring constants between elements are determined by substituting a discrete element model in a linear elastic continuum body. The equations of motion are solved by the explicit time integration method, applied to the elements in succession. Details of the formulation are given in references [1] and [4]. The parameters used in the analysis were fixed in accordance with reference [2].

3 OUTLINE OF IMPACT TEST AND ANALYTICAL MODEL

3.1 Analysis Cases

In this test, target square concrete panels of 150cm side length, and varying from 6 to 35cm in thickness, were subjected to impact by rigid and deformable missiles of diameter 101mm and mass 3.6kgf projected at 215m/sec perpendicular to the panel[3]. Analyses were performed on four cases of panels T180R and T180D with thicknesses 18cm showing different damage modes according to the types of missiles, unperforated panel T300R at 30cm thickness by rigid missile and panel T120D, being 12cm thick and exhibiting perforation mode by deformable missile.

3.2 Analytical model of RC Panel

As shown in Figure 1, an axi-symmetric model comprising, for example, 2083 circular elements for thickness of 30cm (T300R) of 0.50cm radius was used for the analysis. The spring constants, the mass and failure strength for individual elements,and the dynamic increase factor (D.I.F.) dependent on the strain rate effect were determined according to the method adopted in references [2] and [5]. The analysis parameters are shown in Table 1. The Mohr-Coulomb model, with a tension cuttoff law, is applied to the discrete fracture model of concrete. Reinforcements were modelled by considering springs between elements at these locations to possess bi-linear elasto-plastic characteristics. The tensile strength was used for the dynamic yield strength of reinforcement. The time step used in the analysis was set at 2.0×10^{-7} second from the stability conditions for an individual element.

3.3 Analytical model of Missiles

The models of missiles are shown in Figure 2. For the rigid missiles, the steel parts were represented by an axi-symmetric model consisting 15 circular elements 0.50cm in radius and given an infinite strength.

The deformable missiles were represented by a model consisting of 212 elements 0.25cm in radius. The spring constants and strengths were determined as follows to conform to the actual missiles. Normal, shear spring constants (kn, ks) and Compressive, tensile, shear strength(Fc,Ft,Fs) are given by,

$$kn = t \cdot E \cdot 2\pi b/8r \quad (1\text{-a}) \qquad ks = t \cdot E \cdot 2\pi b/4r \quad (1\text{-b})$$

$$Fc = Ft = t \cdot \sigma_u \cdot 2\pi b/2 \quad (2\text{-a}) \qquad ks = t \cdot \sigma_u \cdot 2\pi b \quad (2\text{-b})$$

where E is Young's modulus, t is thickness, r is radius of elements, b is distance form central axis and σ_u is yield strength of material in static analysis and tensile strength in impact analysis.

3.4 Static Compression Analysis of Deformable Missiles

Simulation analysis was conducted on a static compression test of the deformable missiles to verify the validity of the analysis parameters. The analysis parameters are given in Table 2. A comparison of the analysis and test results shows a close agreement in both the load displacement curves and buckling shapes respectively shown in Figures 3 and 4, confirming the appropriateness of the parameters used in the analysis.

4 RESULTS OF IMPACT ANALYSIS

4.1 Damage Modes

The test and analysis results on the final failure conditions to the reinforced concrete panels are compared in Figure 5 to 8. The damage modes showed close agreement in all 4 cases. For panels T300R and T180D, the experimental penetration depths of 39mm and 27mm compared with 42mm and 24mm in the analysis. Comparing the crater diameter of the damage to the panels, in rigid missiles the analysis produced slightly low values for the front and high values for the rear face, while in deformable missiles the analysis showed close agreement with the test results for the front and tended to be smaller for the rear face.

As regards the damage to the missiles, no deformation was observed on the rigid missiles in either the test or the analysis. The missile in case of T180D panel occurred buckling of the front part, followed by symmetrical buckling of the rear part, while buckling of the front part only was observed on the missile for T120D panel; these analysis results are in agreement with the test results.

4.2 Impact Force

Figure 9 shows the impact force at the panel as a result of impact by the missiles. While the impact force was negative at certain points for panel T180R shot by rigid missile, this phenomenon was not observed for T180D panel by deformable missile. The maximum value for the impact force due to the deformable missile was approximately a half of that due to the rigid missile, but the duration time was approximately twice as long, with the result that the impulse was about the same for both cases.

4.3 Penetration and Deformation of Missiles

Figure 10 shows the variation in the penetration depth of missiles. Differences are observed between the rigid and deformable missiles, with the penetration of deformable missiles being smaller in comparison with that of rigid missiles after 0.1msec at which buckling occurred in the front part of deformable missile. The variation in the velocity of missiles after impact shown in Figure 11 indicates that the reduction in the velocity is smaller with deformable missiles after the buckling in the front part of missile. A rapid reduction in missile velocity is observed in the case of T180D after the buckling of the rear part. Figure 12 shows the relationship between impact forces and

displacement of deformable missiles. For panel T180D, where buckling occurs not only in the front part but also in the rear part, a second peak is observed at a deformation of around 14 cm.

4.4 Evaluation of Energy

Figure 13 shows the overall energy transfer for panels T180R and T180D. Major differences were observed in strain energy conditions in missiles and concrete. For T180R panel, because rigid missile does not consume the energy, a large quantity of energy is taken in the concrete, while for panel T180D, the energy is taken by the concrete up to 0.1 msec but there is little increase after this point with most of the energy being consumed through the buckling of the deformable missile.

5 CONCLUSION

1)Quantitative assessment of the buckling strength was achieved in addition to the assessment of the buckling modes in the static compression test simulation of deformable missiles by the DEM, confirming the validity of the method for static compression analysis.

2)Quantitative evaluation of items such as the damage characteristics and penetration of concrete panels and missiles was achieved in the analysis of local damage of reinforced concrete panel due to rigid and deformable missiles by the DEM. The evaluation of the various response values allowed an assessment of the differences in the response characteristics according to the types of missiles.

REFERENCES

[1] Kusano,N., Aoyagi,T., Aizawa,J., Ueno,H., Morikawa,H. and Kobayashi,N. (1991) "Impulsive Local Damage Analysis of Concrete Structure by the Distinct Element Method," Proceedings IMPACT-III, Post-SMiRT 11 Conference, page175-180

[2] Koshika,N., Kusano,N.,Morikawa,H., Aoyagi,T., Kobayashi,N.and Sawamoto,Y.(1992) "Quantitative Estimations of local Damages on concrete Structures under Impulsive Loadings," Proceedings ISIE, International Symposium on Impact Engineering in Sendai

[3] Muto,K. ,Tachikawa,H.,Sugano,T. ,Tsubota,H. ,Kobayashi,H. ,Kasai,Y. ,Koshika,N. Tsujimoto,T. (1989) "Experimental Studies on Local Damage of Reinforced Concrete Structures by the Impact of Deformable Missiles" Proceedings SMiRT 12 Conference

[4] Morikawa,H. and Kobayashi,N. (1992) "Local Fracture Analyses of a Reinforced Concrete Slab by the Discrete Element Method," Proceeding SUSI 92, Second International Conference on Structures Under Shock and Impact in Southampton

[5] Yamaguchi,H. and Fujimoto,K. (1989) "Strain Rate Effect on Dynamic Response of reinforced Concrete Slabs under Impact Loading, "Trans. of Arch. Inst. of Japan No.406, pp25-36

Table 1 Input Parameters of T300R Panel

Concrete unit ;kg,cm

Name	Value	Notes
Normal spring constant Kn	$1.92\times10^5\times2\pi b$	Ref.[1]
Shearspring constant Ks	$0.38\times10^5\times2\pi b$	Ref.[1]
Circular spring constant K_θ	1.18×10^5	$2\pi EA$
Compressive strength Fc	$260\times2\pi b$	considering D.I.F.
Tensile strength Ft	$23.6\times2\pi b$	considering D.I.F.
Cohesion C	$39.2\times2\pi b$	considering D.I.F.
Angle of internal friction ϕ	11.3°	$\mu=0.20$
Mass of particle	$2.64\times10^{-3}\times2\pi b$	Density 2.4 t/m³

Steel

Name	Value	Notes
Spring constant K_B	$2.66\times10^5\times2\pi b$	EA/L
Spring constant $K_{B\theta}$	1.00×10^7	$2\pi EA$
Yield Strength F_B	$779.2\times2\pi b$	Tension Strength
Yeild Strength $F_{B\theta}$	$779.2\times2\pi\times6$	Tension Strength

Table 2 Input Parameters of Deformable Missile

Name	Value Front Part	Value Front Part	Note
Normal spring constant Kn	$1.09\times10^5\times2\pi b$	$1.09\times10^5\times2\pi b$	Eq.(1-a)
Shear spring constant Ks	$2.18\times10^5\times2\pi b$	$2.18\times10^5\times2\pi b$	Eq.(1-b)
Compressive strength Fc	$359\times2\pi b$ ($210\times2\pi b$)	$359\times2\pi b$ ($567\times2\pi b$)	Eq.(2-a) (Static Analysis)
Tensile strength Ft	$359\times2\pi b$ ($210\times2\pi b$)	$359\times2\pi b$ ($567\times2\pi b$)	Eq.(2-a) (Static Analysis)
Shear strength Fs	$719\times2\pi b$ ($420\times2\pi b$)	$1941\times2\pi b$ ($1134\times2\pi b$)	Eq.(2-b) (Static Analysis)

Panel(T300R) Concrete Steel

Number ;2083 fc = 260kg/cm² σ_y = 4560kg/cm²

Radius ;0.50cm v = 0.2 σ_u = 6660kg/cm²

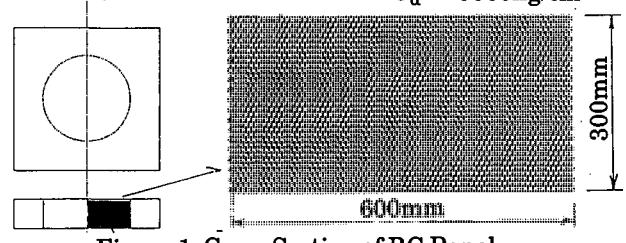

Figure 1 Cross Section of RC Panel

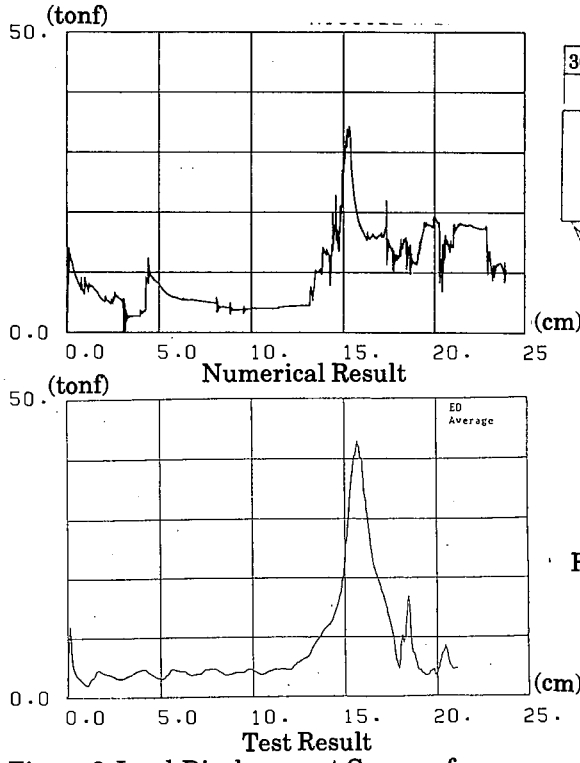

Figure 3 Load-Displacement Curves of Deformable Missiles

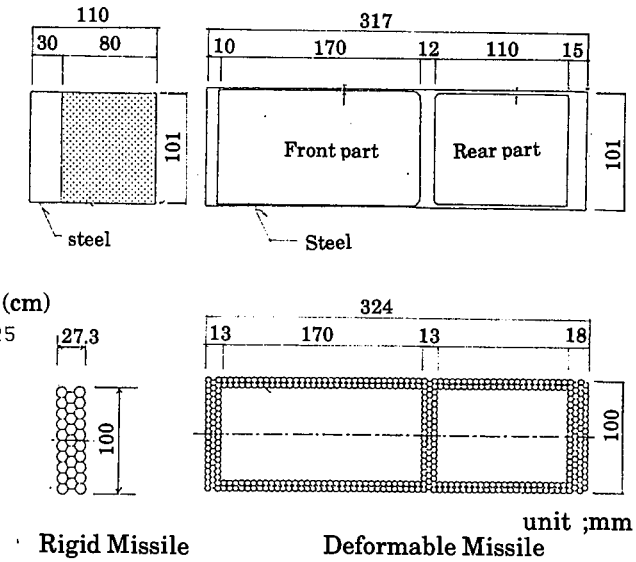

Figure 2 DEM Model of Missiles

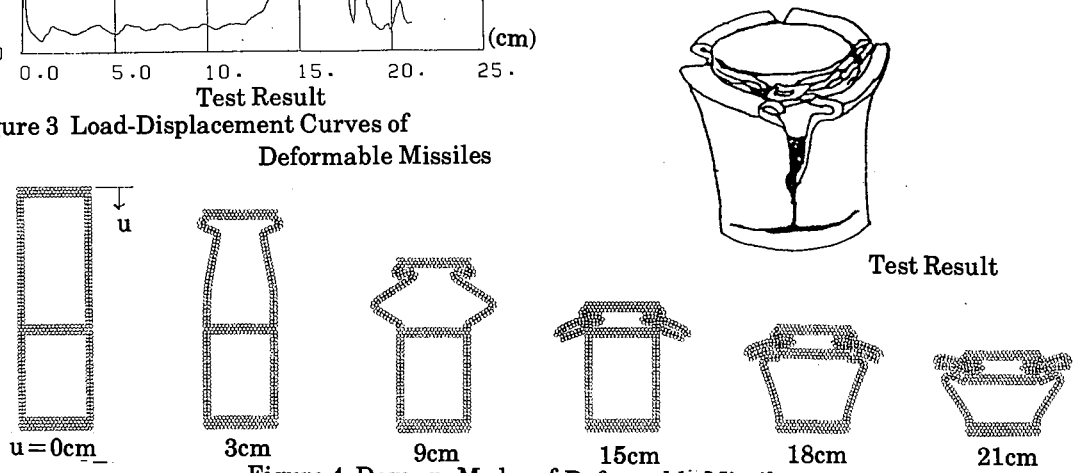

Figure 4 Damage Modes of Deformable Missiles

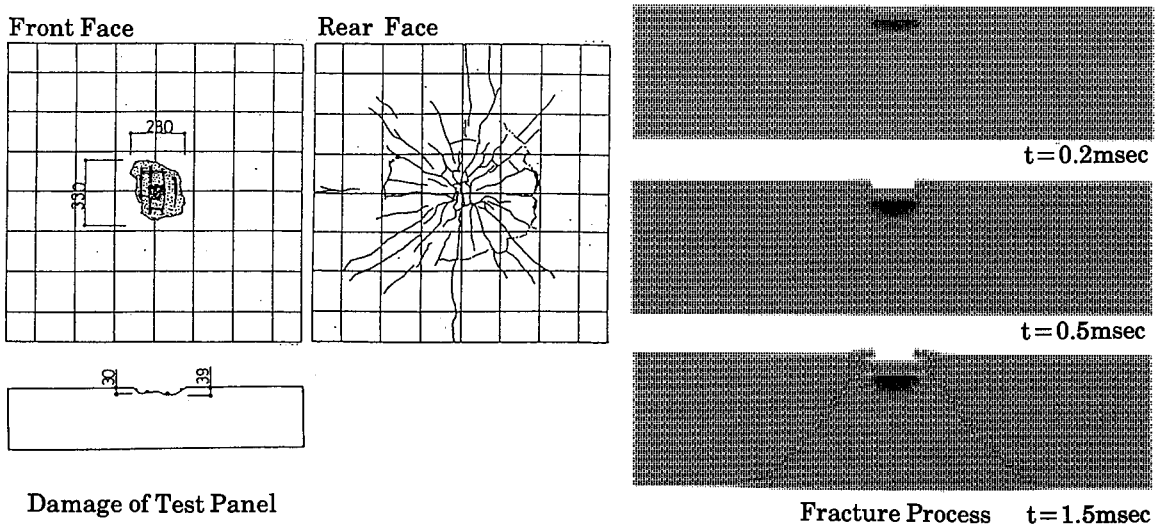

Figure 5 Damage Modes of T300R-Panel

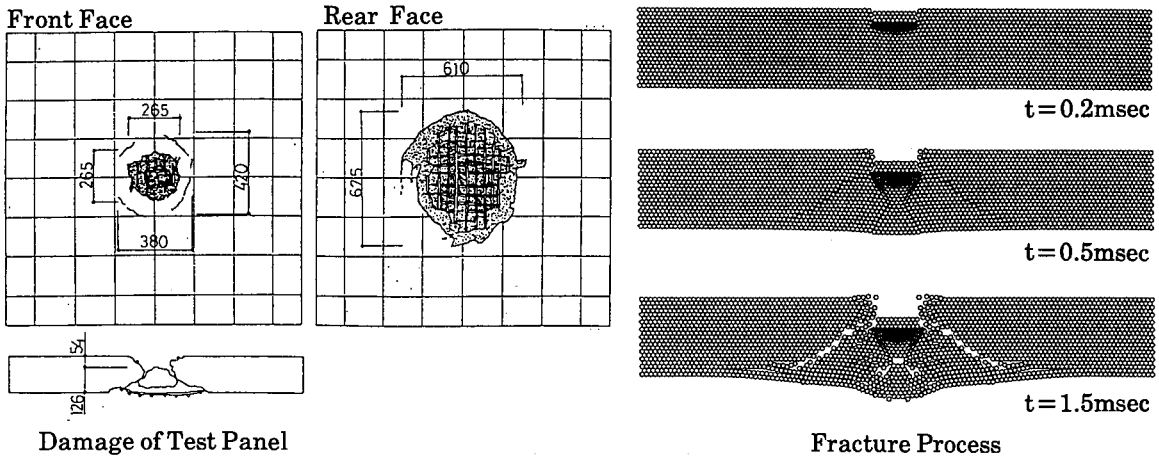

Figure 6 Damage Modes of T180R-Panel

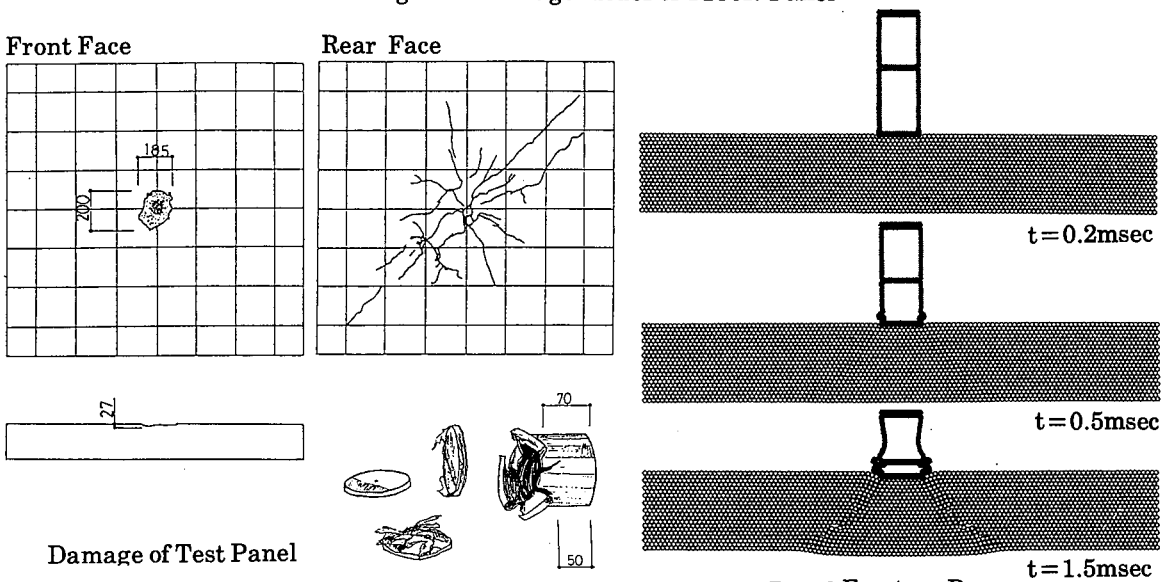

Figure 7 Damage Modes of T180D-Panel Fracture Process

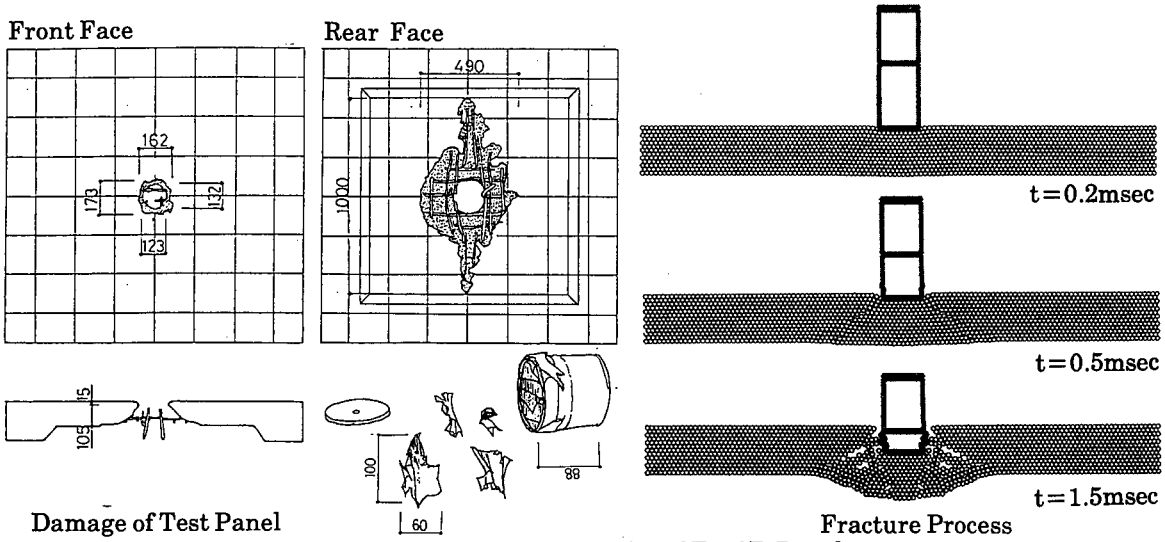

Figure 8 Damage Modes of T120D-Panel

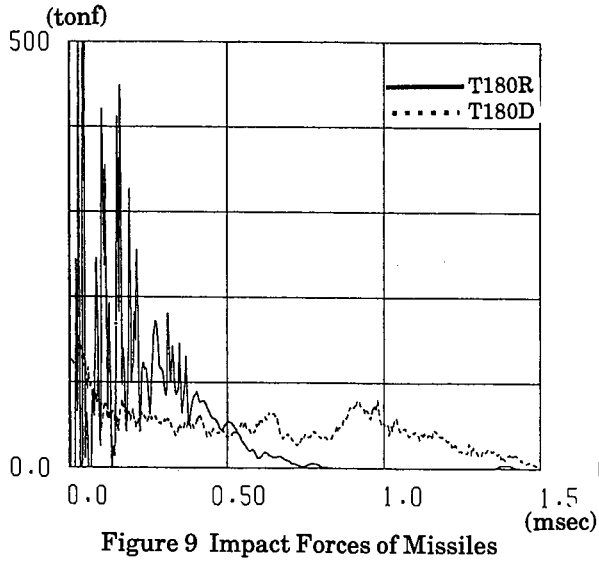

Figure 9 Impact Forces of Missiles

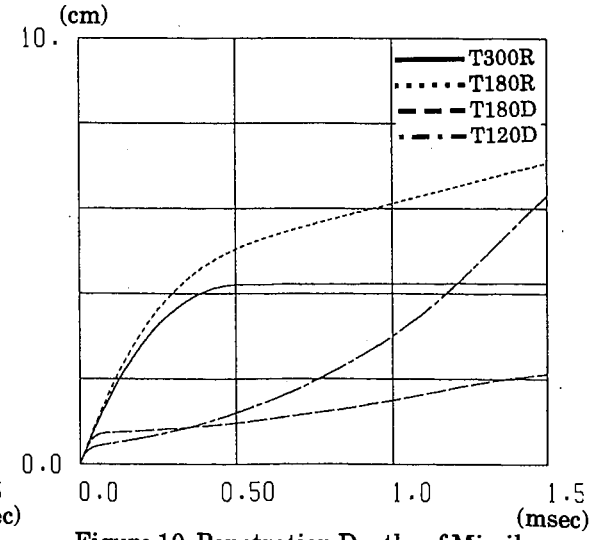

Figure 10 Penetration Depths of Missiles

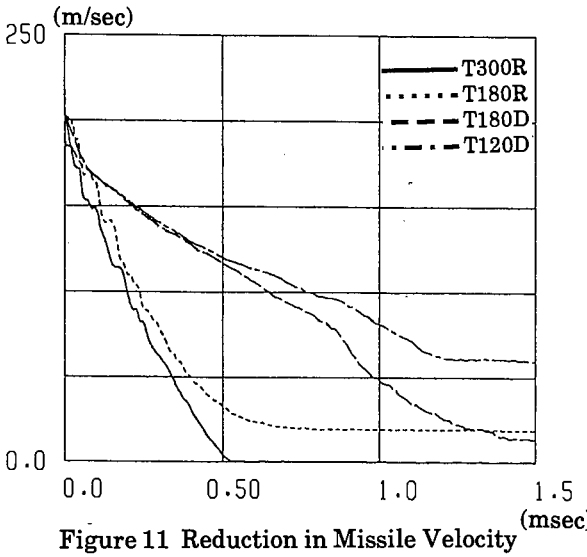

Figure 11 Reduction in Missile Velocity

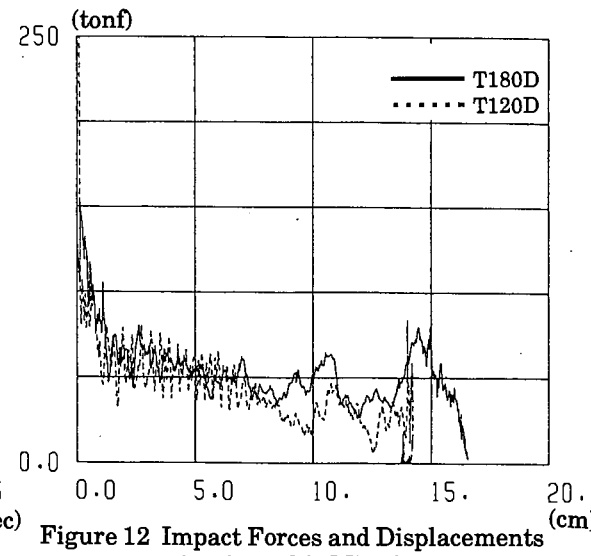

Figure 12 Impact Forces and Displacements of Deformable Missiles

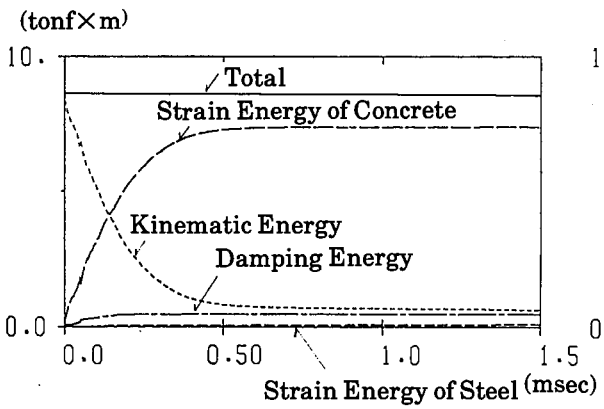

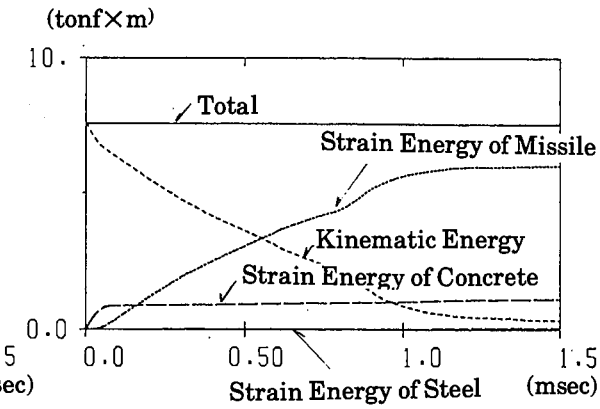

Figure 13 Energy Transfer Process